Supplementary material for

Unveiling unique scaling behavior in miscible, volatile Marangoni spreading.

Anurag Pant* and Baburaj A. Puthenveettil

*Corresponding author. Email: akkupant@gmail.com

S1: Image enhancement.

Image enhancement was done in two sequential steps to improve the visualizations. Initially, instantaneous images underwent noise reduction through a 3×3 pixel median box filter. Each image I_t was subsequently divided into two components: a background image (B_t) representing relatively stationary regions and a foreground image (F_t) encompassing the moving regions. Identification of background regions within (I_t) relied on detecting particle velocities below a specific threshold, notably lower than velocities within the plume regions. This led to the creation of the foreground image using the formula $F_t = I_t - B_t$, where B_t recalculated for each frame, employing a median background subtraction technique (Heyman [3]).

Following this, the instantaneous images underwent temporal averaging across a span of 10 frames (12.5 ms). This averaging process involved the image at a particular instance and the preceding nine frames. The resulting images displayed streaks that depicted particle motion, enabling a clearer visualization of the plume region. One of these time-averaged images is presented as figure 1 in the paper (Heyman [3]).

S2: Drop and substrate properties.

Table S1 presents the properties of ethanol-water and ethanol-water-glycerine drops at various concentrations (C_e) and radii (r_d), including relevant dimensionless numbers associated with the plumes. The drop properties at $25°C$ for different concentrations were obtained from Ernst et al. [2].

C_e (%)	C_g (%)	σ_d (mNm^{-1})	$\Delta\sigma$ (mNm^{-1})	μ_d (cP)	ρ_d (kg m^{-3})	r_d (mm)	ξ	χ	Oh_d (10^{-3})	Bo_d	A	B
20	0	37.97	16.03	1.76	970.36	0.97	1.985	0.97	14.3	0.56	24.12	0.40
40	0	31.00	20.03	2.34	948.47	0.97	2.63	0.95	16.1	0.38	20.60	0.34
60	0	26.00	28.00	2.24	908.72	0.97	2.52	0.91	14.0	0.30	26.5	0.42
80	0	23.80	30.20	1.66	859.58	0.97	1.87	0.86	10.0	0.26	36.5	0.50
100	0	22.00	32.00	1.10	790.74	0.97	1.24	0.79	7.0	0.23	28.57	0.42
100	0	22.00	32.00	1.10	790.74	0.90	1.24	0.79	7.0	0.20	35.24	0.50
100	0	22.00	32.00	1.10	790.74	0.83	1.24	0.79	8.3	0.17	25.21	0.46
60	40	25.4	28.6	5.83	937	1.00	6.55	0.93	35.6	0.32	29.00	0.47

Table S1: Properties of ethanol-water drops at different concentrations and radii, along with relevant dimensionless numbers. Corrections were applied to the surface tension values of water due to the presence of aluminum particles on its surface, accounting for a decrease in the surface tension value. The drop properties at 25°C for varying concentrations were sourced from Ernst et al. [2]. The table includes values of the prefactor A and the exponent B derived from the best-fit curves of r_o versus t for various C_e and r_d values in the drop.

S3. Impact of Evaporation on Observed Phenomena

The rate of evaporation from a planar liquid film, as discussed by [4], is given by:

$$U_e = \frac{\alpha_v}{L}(Ra^2 Ja^3)^{1/5}, \tag{S1}$$

In this equation, the Jacob number (Ja) represents the ratio of sensible heat to latent heat, while the Rayleigh number (Ra) indicates the ratio of buoyancy to dissipative effects. The subscript "v" denotes properties associated with the vapor phase, and L denotes the length of the film. Additionally, λ denotes the latent heat of vaporization, ΔT and $\Delta\rho$ represent the temperature and density differences between the liquid surface and the surroundings, respectively. c_p is the specific heat at constant pressure, α denotes the thermal diffusivity, ν represents the kinematic viscosity, and ρ represents the density.

Similarly, the vertical evaporation velocity (V_e) is expressed as:

$$V_e = U_e \left(\frac{Ja}{Ra}\right)^{1/4} = \frac{\alpha_v}{L}\left(Ra^3 Ja^{17}\right)^{1/20}. \tag{S2}$$

By substituting the properties of ethanol vapor into (S2), including $c_{pv} = 1400$ Jkg^{-1}K^{-1}, $\nu_v = 0.835 \times 10^{-5}$ Nsm^{-2}, $\rho_v = 0.085$ kgm^{-3}, $\lambda_v = 1025 \times 10^3$ Jkg^{-1}, $\beta = 750 \times 10^{-6}$°C^{-1}, $\Delta T \approx 1$°C, and $\alpha_v = 0.00011$ m^{2}s^{-1}, considering a mean film length of $L = 5$mm, the resulting V_e is approximately 4×10^{-5}ms^{-1}. This velocity is approximately three orders of magnitude smaller than the film expansion velocity U_o.

S4. Temporal variation of r_f, l_p and r_o.

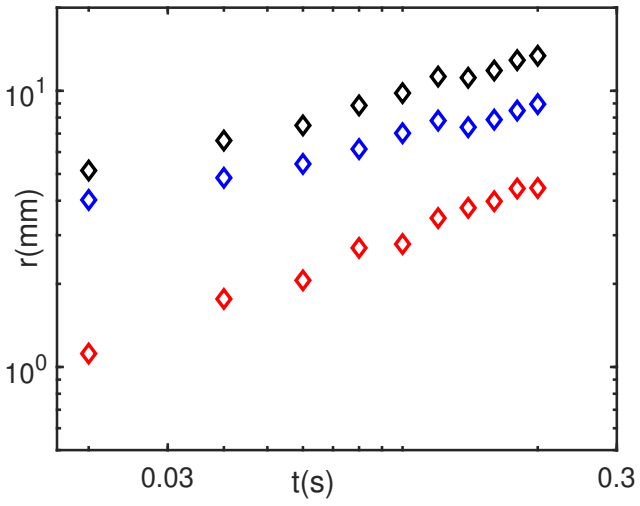

Figure S1: Variation of the film radius r_f, the mean plume length l_p and the mean outer tip radius of the plumes r_o with time, for a drop of $r_d = 0.97$ mm, C_e =60% and C_g =40%. ◊, r_o; ◊, r_f; ◊, l_p.

Figure S1 shows the variation of experimentally measured mean outer tip radius r_o, film radius r_f, and plume length l_p, with time for a drop of $r_d = 0.97$ mm, C_e =60% and C_g =40%. It can be

observed that, at any given instant, r_f is much larger than l_p. However, the plumes grow faster with time, following a power law relationship $l_p \sim t^{3/4}$ (Pant et al. [5]), in comparison to the film radius which varies as $r_f \sim t^{1/4}$ (Dandekar et al. [1]). The mean outer radius r_o at any instant is greater than both r_f and l_p, showing a single power law varying with time, approximately scaling as $r_o \sim t^{1/2}$.

S5. Error in U_o.

We calculate U_o using the relation

$$U_o = ABt^{B-1}, \tag{S3}$$

which is the derivative of the power law fit

$$U_o = At^B, \tag{S4}$$

δU_o, the error in U_o is due to the error in the curve fit and that in t. The error in the curve fit is estimated by calculating the maximum and minimum values of A and B which will fit $r_o \pm \delta r_o$, where δr_o is the known error of 0.3 mm in r_o. From (S3),

$$|\delta U_o| = \left|\frac{dU_o}{dA}\delta A\right| + \left|\frac{dU_o}{dB}\delta B\right| + \left|\frac{dU_o}{dt}\delta t\right|, \tag{S5}$$

where $\delta A, \delta B$ and δt are the errors in A, B and t. Substituting the derivatives from (S5) and rewriting in terms of U_o, we get

$$\left|\frac{\delta U_o}{U_o}\right| = \left|\frac{\delta A}{A}\right| + \left|\frac{\delta B}{B}\right| + \left|(B-1)\frac{\delta t}{t}\right| + |\delta B \ln t|. \tag{S6}$$

For example, in the case of $C_e = 100\%$ and $r_d = 0.97$mm, $A = 27, B = 0.4$, $\delta A = 1$, $\delta B = 0.02$, $\delta t = 0.0033$s. Using these values in (S6) we obtain the errors in U_o at various time instants; these errors are shown in figure 4(b), and the dependent errors are shown in figure 5(b), as vertical error bars.

References

[1] Dandekar, R., Pant, A., and Puthenveettil, B. A. (2017). Film spreading from a miscible drop on a deep liquid layer. *Journal of Fluid Mechanics*, 829:304—-327.

[2] Ernst, R., Watkins, C., and Ruwe, H. (2002). The physical properties of the ternary system ethyl alcohol–glycerin–water. *The Journal of Physical Chemistry*, 40(5):627–635.

[3] Heyman, J. (2019). Tractrac: A fast multi-object tracking algorithm for motion estimation. *Computers & Geosciences*, 128:11–18.

[4] Lock, G. S. H. (1996). *Latent heat transfer: an introduction to fundamentals*. Number 43. Oxford University Press.

[5] Pant, A., Puthenveettil, B. A., and Kalpathy, S. K. (2023). Marangoni plumes in miscible spreading. *Physics of Fluids*, 35(3):032107.